

Original

Hedayati, M.K.; Zillohu, A.U.; Strunskus, T.; Faupel, F.; Elbahri, M.:
**Plasmonic tunable metamaterial absorber as ultraviolet
protection film**
In: Applied Physics Letters (2014) AIP

DOI: 10.1063/1.4863202

Plasmonic tunable metamaterial absorber as ultraviolet protection film

M. K. Hedayati,¹ A. U. Zillohu,² T. Strunskus,³ F. Faupel,³ and M. Elbahri^{1,2,a)}

¹Nanochemistry and Nanoengineering, Institute for Materials Science, Faculty of Engineering, Christian-Albrechts-Universität zu Kiel, Kaiserstrasse 2, 24143 Kiel, Germany

²Nanochemistry and Nanoengineering, Institute of Polymer Research, Helmholtz-Zentrum Geesthacht, Max-Planck-Str. 1, 21502 Geesthacht, Germany

³Chair for Multicomponent Materials, Institute for Materials Science, Faculty of Engineering, Christian-Albrechts-Universität zu Kiel, Kaiserstrasse 2, 24143 Kiel, Germany

(Received 8 October 2013; accepted 10 January 2014; published online 27 January 2014)

Plasmonic metamaterials designed for optical frequency have to be shrunk down to few 10th of nanometer which turns their manufacturing cumbersome. Here, we shift the performance of metamaterial down to ultraviolet (UV) by using ultrathin nanocomposite as a tunable plasmonic metamaterial fabricated with tandem co-deposition. It provides the possibility to realize a plasmonic metamaterial absorber for UV frequency with marginal angle sensitivity. Its resonance frequency and intensity can be adjusted by changing thickness and filling factor of the composite. Presented approach for tunable metamaterials for high frequency could pave the way for their application for thermo-photovoltaic, stealth technology, and UV-protective coating.

© 2014 AIP Publishing LLC. [<http://dx.doi.org/10.1063/1.4863202>]

Plasmonic metamaterials (PMs) as a class of materials with some exotic properties drawn the attention considerably in the last decade due to non-limited potential for vast number of applications such as negative refractive index,¹ nanolaser,² and photovoltaics³ amongst others. Metals, as a core of majority of PM, suffer from losses especially when it is supposed to be contrived for ultraviolet (UV)-visible frequencies.⁴ For a metal surrounded by an ideal dielectric, loss is originated by free-electron scattering in the metal and, at high frequencies, through absorption via inter-band transitions.⁵ In spite of early consideration of loss as a foremost drawback of PM, the absorptivity is started to be considered as one of the new potential application of PM following the first experimental demonstration of metamaterial perfect absorber (MPA)⁶ (For details, see the review by Padilla and co-workers⁷).

Thick film of metal-dielectric^{8–10} or semiconductor-dielectric¹¹ composite have been used as spectrally selective absorber since late 70th for solar thermal absorber, whereas the high absorption in metallic composite was attributed to the interband transition of metal and small particle resonance.^{9,10} Because of the large thickness of these films, their application in miniaturized device of 21st century is limited. Replacing small inclusion of nanocomposite with lithographically fabricated nanostructure has been the main trend in development of recent MPA. This approach could realize perfect absorber but due to the narrow band-width, sensitivity to the angle of incidence, and low production tolerance of this complicated structure, their performance could not exceed that of old hybrid films. We have shown recently that instead of using very thick composite, ultra thin film deposited on highly reflecting mirror where the two layers separated with a dielectric layer could act as a super absorber for different frequencies.^{12,13} This approach is enjoying ease of

fabrication, low production cost and possessing high efficiency in the sense of absorption intensity, band-width, and angular sensitivity while being ultrathin (20 nm). In such a plasmonic metamaterial super absorber (PMSA), the absorption is routed from several sources: multi-reflection of light from the base mirror which results in multi-excitation of plasmon resonance in particles, destructive interference between the thin layer which (increases) reduces the reflectivity (absorption)¹⁴ and strong light confinement (creation of hot spot) between the small gaps of particles.¹²

In general, excluding few exceptions, gold is the leading metallic components of metamaterials in general and metamaterial absorber, in particular, because of its large (plasmonic) absorption in green part of visible.^{12,15–19} However, the perfect absorption frequency is mainly limited to visible/near infrared²⁰ and shifting the resonance to shorter wavelength (e.g., UV) remains as a challenge. Because of inter-band transitions frequency of silver (in UV region) and its short-wavelength plasmon resonance, silver based perfect absorber can be a promising candidate for high efficient inorganic UV protection layer. In fact, any surface plasmon wave (SPW) propagating along the surface of gold is more attenuated and exhibits higher localization of electromagnetic field in the dielectric than an SPW supported by silver.²¹ Therefore, the silver base PM cannot only be more practical for energy absorption but also the light can propagate in metal/dielectric interface for larger distance than that of gold.²²

UV radiation is typically categorized into 3 bands in sequence of rising energy: UV-A (320–400 nm), UV-B (280–320 nm), and UV-C (100–280 nm). This division was put forward by the Commission Internationale de l'Eclairage (CIE) and corresponds broadly to the effects of UV radiation on biological tissue. Indeed, approximately 5% of the ground-level solar radiation is ultraviolet radiation, mostly in the UV-A range.²³ Accordingly, a practical UV coating layer should be more absorbing in UV-A frequencies. Here, in this

^{a)} Author to whom correspondence should be addressed. Electronic mail: me@tf.uni-kiel.de

report, we design and fabricate a tunable silver-SiO₂ nanocomposite following our recent works^{12,13} on a highly reflecting substrate by tandem co-deposition to realize a PMSA which operates through the visible up to UV-A frequency. SiO₂ film as a dielectric used to separate the composite from the base mirror. In this configuration, the huge absorption of light in a broad range of frequency (in visible and UV) can be achieved which surpassing the absorption intensity of recently reported silver absorber.^{24–26} The absorption of presented structure is almost invariant to the angle of incident and its broadband peak can be tuned throughout the UV-visible frequencies, which shows its great potential in sensing applications, too.²⁷

To demonstrate the feasibility of our absorber functioning as a UV protective layer, we compare the performance of current design with organic counterpart. For that purpose, a dye-molecule incorporated in polymer matrix film²⁸ was deposited on optically thick silver film as UV absorber, and the absorption intensity and band-width of the both film were collated. It turns out that the absorption intensity of PMSA system is twice of organic one. Not only the absorption intensity of silver base absorber is higher but also its bandwidth cover broader range of frequency than the single-band dye absorber showing its advantage over traditional absorbers.²⁹

A cylindrical custom-build vacuum chamber was used for sputtering of the metal and dielectric. By two magnetrons with an angle of 50°, co-sputtering was done in order to make a nanocomposite. Simultaneous sputtering from different sources allows deposition of nanocomposites with different filling factors (ff) and thicknesses. For acquiring a homogeneous thickness for the film and uniform dispersion of metals, all depositions were carried out on the samples attaching to a rotatable holder.³⁰ Spirophenanthrooxazine (SPO) molecules (1,3-Dihydro-1,3,3-trimethylspiro[2H-indole-2,3'-[3H]phenanthr[9,10-b](1,4)oxazine]), which was used as a photochromic dye, was obtained from Sigma Aldrich. For spin coating a thin layer of SPO doped Polystyrene (PS), 1.2 wt. % of solute, consisting of equal amounts of PS and SPO, was dissolved in toluene. Substrate was hold in vacuum chuck of the spin coater and 70 μ l of the desired solution was injected on its surface. The spinning speed of 2000 rpm used for samples to yield a uniform thin film. Thickness measurements were performed using the Dectak 8000 profilometer, and optical analysis was done by a UV-Vis-NIR spectrometer (Lambda 900, Perkin Elmer). Angular reflection measurements of the films were carried out with J. Woolam M-2000 (spectroscopic ellipsometer).

The elemental map of the real sample measured with HRTEM and the schematic geometry of the designed PMSA are presented in Figures 1(a) and 1(b), correspondingly. The stack is composed of 4 layers. From bottom to up, glass, 200 nm Silver film, 10–30 nm SiO₂, and 20 nm Silver-SiO₂ composite, respectively. The gap between the nanoparticles (NPs) is very small because of high filling factor of particles. Indeed, the inter-particle distance is varying between 2 nm and 5 nm which guarantees the strong confinement of electric field in such a system. Since the base layer is optically thick (200 nm silver), the transmission is nearly zero and hence reducing the reflectivity to very negligible amount would provide the condition for super absorption.

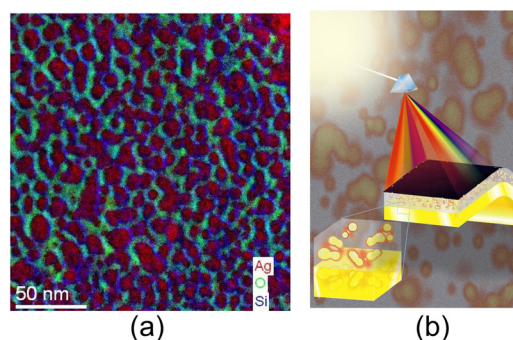


FIG. 1. (a) TEM elemental map of the optimized silver-SiO₂ nanocomposite for perfect absorption. (b) Schematic of the geometry of the metamaterials where the base layer is a optically thick silver covered with 15 nm SiO₂ film. Atop, 15 nm Ag-SiO₂ composite with near percolation filling factor is deposited.

It is known that silver's reflection is close to 100% over the entire visible region but it reduces to less than 10% in 320 nm due to a surface plasmon resonance.³¹ Hence, the absorption of optically thick Ag film is usually below 5% in the visible region.²⁴ On the other hand, the transparency of Silver-SiO₂ composite with 30%–40% ff is around 44% in visible, but its average reflection is 25%. In Figure 2(a), transmission and reflection spectra of the 20 nm Silver-SiO₂ composite with 40% ff of metallic particles are depicted. The dissimilarity between the transmission and reflection spectra in Figure 2(a) could be due to the fact that the transmission spectra which reflect the morphology of the films throughout their depth are more affected by particle aggregation, but reflection spectra are more sensitive to surface structures in the film.³² The drop in the transmission of composite film stem from the localized particle plasmon resonance (LPPR) of silver particles which revealed at 450 nm. In spite of known sharp resonance peak of silver particle, the dip in spectra of nanocomposite is relatively wide which originate from different shape and size (distribution of particles in sizes)²⁴ of the particles as well as dipole-dipole interaction within the matrix.¹² The reflection spectra show a broad resonance, too. The appearance of a wide reflection peak at the plasmon frequency illustrates that the composite reflects the light at near resonance wavelength. This can be ascribed to the semi-metallic structure (surface morphology) of high filling factor composite which reflects the light through the visible. Indeed, the intrinsic reflection of composite film provides the condition of Fabry-Perot cavity formation when they are come to proximity of a reflective mirror (which is discussed in the following).

It is known that metallic particles in air have a different optical property than of metal-dielectric nanocomposite. The resonance red-shift when the refractive index of the adjacent dielectric increases. This effect is more pronounced once the particle is come within reach of a metallic substrate.³³ In other words, when a dielectric envelop the isolated metallic nanoparticle, the induced screening charges on the metal-dielectric interface lower the plasmon excitation energy ensuing in red-shifting of the resonance. Similarly, for coupled nanoparticles, the dielectric materials also screen and weaken the interaction between metal nanoparticles and decrease the shift of the coupled plasmon.³⁴ According to the mentioned reason, we

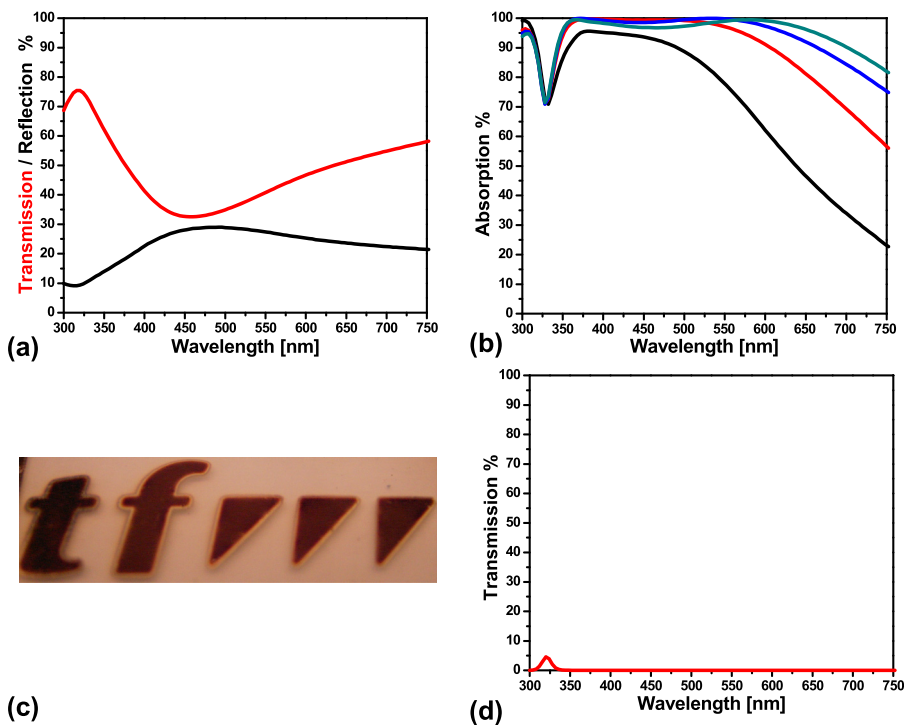


FIG. 2. (a) Reflection and transmission spectra of 20 nm silver-SiO₂ nanocomposite with 40% filling factor deposited on glass substrate. (b) Absorption spectra of silver-SiO₂ nanocomposite with 15 nm (black curve), 20 nm (red curve), 25 nm (blue curve), and 30 nm (green curve) thickness deposited on 15 nm SiO₂ coated silver mirror. (c) True color photograph of the perfect absorber coated on transparent polymeric substrate presenting the logo of Faculty of Engineering (TF) of University of Kiel. (d) Transmission spectra of typical perfect absorber.

are able to shift the resonance peak of Ag from UV to visible by depositing silver-SiO₂ nanocomposite atop of a mirror. Beside the particles coupling inside the composite, the resonance further red-shifts due to the fact that the particle dipole is anti-symmetrically coupled to its image inside the silver mirror.³³

In addition to the plasmonic absorption of ensembles of particles (i.e., nanocomposite), interference also contribute to its low reflectivity.¹⁴ In such a stack of layers (nanostructure and continuous metallic film), the reflection reduction is achieved due the impedance matching of the system and air. On other hand, the Fabry-Perot cavity is created between the top composite and the bottom mirror leading to strong interference between the incident and the reflected wave. In other words, the superposition of the multiple reflections from the base layer destructively interferes with the direct reflection from the air-composite interface. With the optimized interlayer thickness, these two waves counteract each other ensuing in zero reflection; whereas with other spacer thicknesses (Figure 2(b)) the amplitude and phase do not or partially match, leading to a less intense absorption peak and subsequent frequency shift.³⁵ As mentioned above, in spite of the narrow resonance band of silver, the composite has a broad resonance width due to the dispersive size of the particles and particle-particle (dipole-dipole) interaction within the layer. Apart from these effects, deviation from perfect spherical shape could profoundly influence the large broadening.³⁶ Therefore, the cavity resonance is occurred at several wavelength leading to vanishing of reflection in a broad range of frequency. Since the base layer is optically thick, no light transmit through the layers and consequently super absorption is achieved.

In contrast to other reported composite-based super absorbers, the presented silver base PMSA is unique since the absorption intensity is reaching 100% in UV (up to green

part of visible) which is the first PMSA reported for such a high frequency (UV-A wavelength). The film appearance is dark-red demonstrating that this PMSA is highly reflecting at red part of spectra (Figure 2(c)).

Macroscopically consideration of the system shows that the absorption band is split into two separate (broad) peaks similar to the stacks of silver cluster and mirror.¹⁴ We attribute the resonance at shorter wavelength (around 360 nm) to the silver interband transition. Indeed, the interband transition from occupied *d* states to unoccupied *p* and *s* states above Fermi level appears at 310 nm and 350 nm in bulk silver, correspondingly. But, for silver nanostructures such an electron transitions could occur above 350 nm wavelength and depend on nanostructure geometry.²⁴ The second broad peak which appears at longer wavelength might stem from localized surface plasmon resonance of the silver particles (~370 nm) and interference (550–600 nm). This becomes more apparent when the thickness of the composite changes. In Figure 2(b), the absorption spectra of silver-SiO₂ nanocomposite with 15 nm, 20 nm, 25 nm, and 30 nm thickness are shown. The low frequency peak position red-shift with thickening the film which is a sign that the peak is interference routed.¹⁴ Moreover, the peak itself split into two parts as long as the composite thickness raises from 10 to 30 nm. Further thickening of the composite results in a drop in the absorption in visible and hence reduce the efficiency of the system, though it further broaden the spectra.

Beside of the two mentioned wide-band peak, a dip in absorption spectra reveals at very short wavelength (around 325 nm). From the first glance, it might be concluded that this dip is routed from the small transmission of silver film at 320 nm (Figure 2(d)). But the drop intensity is around 30% meaning 10 times bigger than the transmission intensity of film.

It is known that surface plasmon resonance can be excited on the silver film at around 340 nm due to the

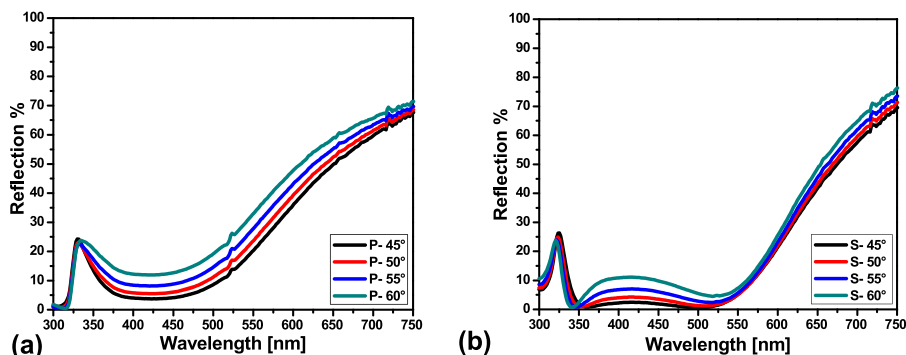


FIG. 3. Reflection spectra of 20 nm silver-SiO₂ nanocomposite with 30% filling factor deposited on 20 nm SiO₂ coated silver film (200 nm thick). (a) -p and (b) -s polarization at different angle of incidence.

roughness originated from deposition.^{37,38} Therefore, the reflection spectra of the stacks will show two dips at higher frequency; One at 320 associated with the plasma frequency of silver and the second one at around 340 nm corresponding to the surface plasmon resonance of the bulk silver. In other words, two reflection dips reveal in the spectra of silver mirror one at 340 and the other one at 320 nm. Therefore, the mentioned drop (reflection peak) in the absorption is the boundary of two resonance phenomenon which occurred in the present multi-stack.^{39,40}

Reflection measurement at different angle of incidence with two different polarizations (-s and -p) (Figure 3) showed that the current PMSA is almost angle and polarization invariant. The reflection intensity stay low for both polarization even at high incidence angle (60°) demonstrating that the performance of such a PMSA is not being influenced considerably by angle of incidence. Nevertheless, there is a slight difference in s- and p-polarization that we attributed to the Brewster angle. Generally, the s-polarized reflection in a metamaterials can reach to zero at higher angle of incidence provided that the permeability of the materials is non-unity.⁴¹ Since the permeability of current metamaterial is not unity in visible regime;¹² therefore, the reflection is vanishing for s-polarization at certain frequency while p-polarized light slightly reflect-off the surface.

Alteration of ff is an other fundamental parameters which can tune the optical response of this PMSA. Figure 4(a) shows the absorption spectra of the Silver-SiO₂ nanocomposite with different filling factors while the other parameters kept constant. As long as the ff increases, the spectra red-shift and its band broadens. However, above the certain composition (optimized value), the absorption band starts to shrink again. The above shift could be attributed to the amplified electromagnetic interaction among the particles in addition to the change in the effective permittivity of the surrounding medium as predicted by Maxwell-Garnett theory.³⁶ For our developed system, it seems that 42% ff show the best performance and the width of the absorption peak (with intensity higher than 95%) becomes 220 nm (Figure 4(b)).

In the current PMSA, the sensitivity of the absorption intensity to the filling factor variation is less than the thickness. We attribute the mentioned difference to the limited range of filling factor variation. On other hand, the region of near percolation is very restricted, and a little increment of the metal ratio leads to the metallic behavior of composite and therefore the reflection increment (absorption drop) of the stack.¹² Around the percolation threshold (around 50%), the peak broadening starts to decrease (Figure 4(a) (olive curve)) prior to dropping sharply after percolation. This is owing to the decline in scattering of the conduction electrons

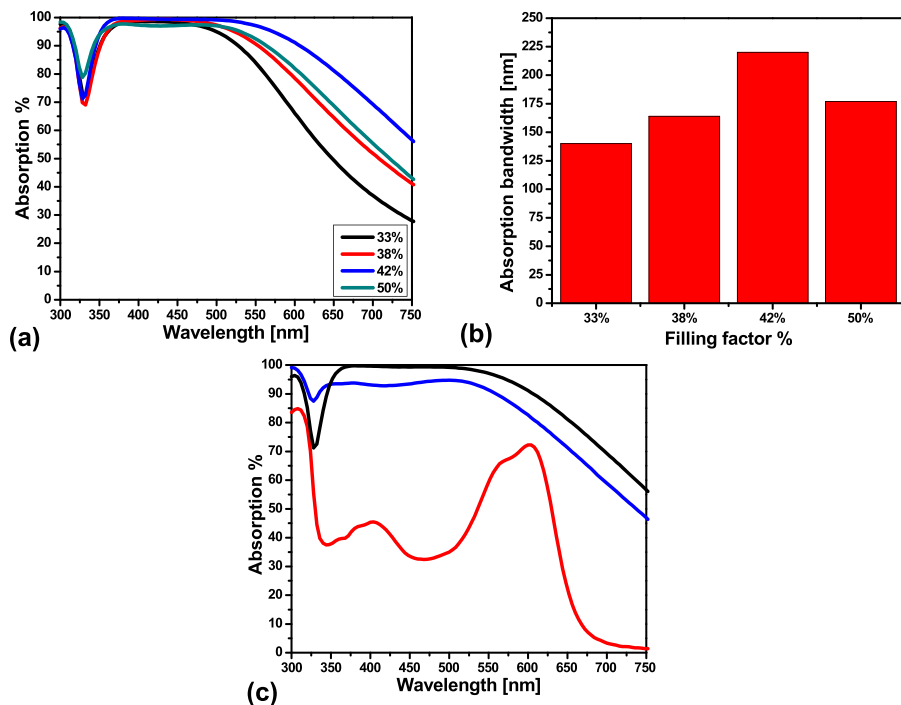


FIG. 4. (a) Absorption spectra of silver-SiO₂ nanocomposite with different filling factors. (b) Absorption band-width with intensity greater than 95% for different PMSA with variety of filling factor shown in (a). (c) Absorption spectra 200nm silver film coated with 40 nm polystyrene-SPO composite (red curve) and 20 nm silver-SiO₂ nanocomposite with 42% filling factor deposited on 10 nm (blue curve) and 15 (black curve) nm SiO₂ film. The organic film is UV illuminated prior to measurement.

by surfaces and discontinuities.⁴² In other words, the high ff only could give rise to high absorption provided that the particles are discontinuous and do not make any metallic chains in the matrix. In fact, incorporation of solid dielectric between the particles (for formation of composite) provides the chance to keep them distant from others and delay the interconnection up to relatively high ff of metals.

In order to prove the better performance of the current PMSA compared to the known dye UV absorber, polystyrene film doped with spirooxazine molecules were spin coated on 200 nm thick silver film. Based on the optimization experiments, the most intense absorption can be realized when the thickness of the coating is around 40 nm and its highly concentrated (~50% SPO). The absorption spectra of the silver absorber and UV irradiated organic coating are depicted in Figure 4(c). It is clear that the absorption intensity as well as band-width of silver PMSA is larger than its organic counterpart. Indeed, the average absorption of the doped polystyrene in the UV-A range is (45%) half of the absorption intensity of the silver absorber (92%) further showing that the PMSA can be a higher efficiency alternative for organic UV protection layer. It is worth mentioning that the absorption dip in high frequency (in PMSA) can be reduced by thinning the spacer layer down to 10 nm but in the expense of overall absorption reduction (in otherwise wavelengths). In other words, one can compensate the drop and increase the absorption intensity up to 90% at 325 nm by thinning the spacer layer (Figure 4(c) (blue curve)).

We believe that the presented perfect absorber might pave the way of metamaterials application for thermo-photo-voltaic,⁴³ stealth technology,⁴⁴ and UV-protective coating.²³

Note that the long-term stability of silver is rather poor.^{21,45} Indeed, oxygen or water could penetrate even dense silica matrices on a scale of days, not only through pores but even through the matrix network and deteriorate its optical properties.⁴⁶ Therefore, more efforts and improvements are needed to upscale the fabrication of the present PMSA for long term performance.

In summary, a plasmonic tunable metamaterial absorber is presented for UV part of spectrum. The absorption frequency and intensity of the metamaterial are considerably tuned throughout the UV-visible wavelengths. We achieved this unprecedented level of wavelength and intensity agility by varying the nanoparticle volume fraction, composite, and spacer layer thickness. It was shown that the absorption of silver PMSA is twice of organic absorber in UV and visible range. Therefore, this class of metamaterial could be a promising candidate for highly UV and visible absorbing coatings.

We would like to acknowledge C.V.S. Chakravadhanula for TEM imaging and A. Tavassolizadeh for drawing the sketch. We gratefully acknowledge the financial support by the German Research Foundation (DFG) through the projects SFB 677 (C1,C9) and EL 554/1-1. M. E. would like to thank the Initiative and Networking Fund of the Helmholtz Association's (grant No. VH-NG-523) for providing the financial base for the start-up of his research group.

¹A. Boltasseva and V. M. Shalaev, *Metamaterials* **2**, 1 (2008).

²A. K. Sarychev and G. Tartakovskiy, *Phys. Rev. B* **75**, 085436 (2007).

³H. A. Atwater and A. Polman, *Nature Mater.* **9**, 205 (2010).

⁴R. F. Oulton, *Mater. Today* **15**, 26 (2012).

⁵P. Berini and I. De Leon, *Nat. Photonics* **6**, 16 (2012).

⁶N. I. Landy, S. Sajuyigbe, J. J. Mock, D. R. Smith, and W. J. Padilla, *Phys. Rev. Lett.* **100**, 207402 (2008).

⁷C. M. Watts, X. Liu, and W. J. Padilla, *Adv. Mater.* **24**, OP98 (2012).

⁸J. C. C. Fan and P. M. Zavracky, *Appl. Phys. Lett.* **29**, 478 (1976).

⁹H. G. Craighead and R. A. Buhrman, *Appl. Phys. Lett.* **31**, 423 (1977).

¹⁰H. G. Craighead and R. A. Buhrman, *J. Vac. Sci. Technol.* **15**, 269 (1978).

¹¹J. I. Gittleman, *Appl. Phys. Lett.* **28**, 370 (1976).

¹²M. K. Hedayati, M. Javaherirahim, B. Mozooni, R. Abdelaziz, A. Tavassolizadeh, V. S. K. Chakravadhanula, V. Zaporozhchenko, T. Strunkus, F. Faupel, and M. Elbahri, *Adv. Mater.* **23**, 5410 (2011).

¹³M. K. Hedayati, F. Faupel, and M. Elbahri, *Appl. Phys. A* **109**, 769 (2012).

¹⁴A. Leitner, Z. Zhao, H. Brunner, F. R. Aussenegg, and A. Wokaun, *Appl. Opt.* **32**, 102 (1993).

¹⁵J. Dai, F. Ye, Y. Chen, M. Muhammed, M. Qiu, and M. Yan, *Opt. Express* **21**, 6697 (2013).

¹⁶C. Hu, Z. Zhao, X. Chen, and X. Luo, *Opt. Express* **17**, 11039 (2009).

¹⁷C. Hu, L. Liu, Z. Zhao, X. Chen, and X. Luo, *Opt. Express* **17**, 16745 (2009).

¹⁸M. G. Nielsen, A. Pors, O. Albrektsen, and S. I. Bozhevolnyi, *Opt. Express* **20**, 13311 (2012).

¹⁹P. Ding, E. Liang, G. Cai, W. Hu, C. Fan, and Q. Xue, *J. Opt.* **13**, 075005 (2011).

²⁰X. Chen, H. Gong, S. Dai, D. Zhao, Y. Yang, Q. Li, and M. Qiu, *Opt. Lett.* **38**, 2247 (2013).

²¹J. Homola, S. S. Yee, and G. Gauglitz, *Sens. Actuators B* **54**, 3 (1999).

²²B. Lamprecht, J. R. Krenn, G. Schider, H. Ditlbacher, M. Salerno, N. Felidj, A. Leitner, F. R. Aussenegg, and J. C. Weeber, *Appl. Phys. Lett.* **79**, 51 (2001).

²³M. Zayat, P. Garcia-Parejo, and D. Levy, *Chem. Soc. Rev.* **36**, 1270 (2007).

²⁴V. G. Kravets, S. Neubeck, A. N. Grigorenko, and A. F. Kravets, *Phys. Rev. B* **81**, 165401 (2010).

²⁵A. Moreau, C. Ciraci, J. J. Mock, R. T. Hill, Q. Wang, B. J. Wiley, A. Chilkoti, and D. R. Smith, *Nature* **492**, 86 (2012).

²⁶K. Aydin, V. E. Ferry, R. M. Briggs, and H. A. Atwater, *Nature Commun.* **2**, 517 (2011).

²⁷T. R. Jensen, M. D. Malinsky, C. L. Haynes, and R. P. Van Duyne, *J. Phys. Chem. B* **104**, 10549 (2000).

²⁸M. Jamali, M. K. Hedayati, B. Mozooni, M. Javaherirahim, R. Abdelaziz, A. U. Zillohu, and M. Elbahri, *Adv. Mater.* **23**, 4243 (2011).

²⁹B. Mahtig, H. Böttcher, K. Rauch, U. Dieckmann, R. Nitsche, and T. Fritz, *Thin Solid Films* **485**, 108 (2005).

³⁰M. Elbahri, M. K. Hedayati, K. S. V. Chakravadhanula, M. Jamali, T. Strunkus, V. Zaporozhchenko, and F. Faupel, *Adv. Mater.* **23**, 1993 (2011).

³¹N. L. Thomas and J. D. Wolfe, *Proc. SPIE* **4003**, 312 (2000).

³²Y. Saito, J. J. Wang, D. N. Batchelder, and D. A. Smith, *Langmuir* **19**, 6857 (2003).

³³G. Lévêque and O. J. F. Martin, *Opt. Express* **14**, 9971 (2006).

³⁴B.-h. Choi, H.-H. Lee, S. Jin, S. Chun, and S.-H. Kim, *Nanotechnology* **18**, 075706 (2007).

³⁵H.-T. Chen, *Opt. Express* **20**, 7165 (2012).

³⁶S. K. Mandal, R. K. Roy, and A. K. Pal, *J. Phys. D: Appl. Phys.* **35**, 2198 (2002).

³⁷T. Huen, G. B. Irani, and F. Wooten, *Appl. Opt.* **10**, 552 (1971).

³⁸P. Taneja, P. Ayyub, and R. Chandra, *Phys. Rev. B* **65**, 245412 (2002).

³⁹N. Liu, H. Guo, L. Fu, S. Kaiser, H. Schweizer, and H. Giessen, *Adv. Mater.* **19**, 3628 (2007).

⁴⁰J. Hao, J. Wang, X. Liu, W. J. Padilla, L. Zhou, and M. Qiu, *Appl. Phys. Lett.* **96**, 251104 (2010).

⁴¹R. Watanabe, M. Iwanaga, and T. Ishihara, *Phys. Status Solidi B* **245**, 2696 (2008).

⁴²T. W. H. Oates and A. Mücklich, *Nanotechnology* **16**, 2606 (2005).

⁴³J.-B. Brückner, J. Le Rouzo, L. Escoubas, G. Berginc, O. Calvo-Perez, N. Vukadinovic, and F. Flory, *Opt. Express* **21**, 16992 (2013).

⁴⁴N. Engheta, "Thin absorbing screens using metamaterial surfaces," paper presented at the *IEEE Antennas and Propagation Society International Symposium*, 2002.

⁴⁵B. D. Gupta and R. K. Verma, *J. Sens.* **2009**, 979761 (2009).

⁴⁶M. Hillenkamp, G. D. Domenicantonio, O. Eugster, and C. Félix, *Nanotechnology* **18**, 015702 (2007).